Proceedings of PVP2006-ICPVT-11
2006 ASME Pressure Vessels and Piping Division Conference
July 23-27, 2006, Vancoucer, BC, Canada

PVP2006-ICPVT-11-93539

GOVERNING EQUATIONS OF MOTION OF WALKING BEHAVIOR OF UNANCHORED FLAT-BOTTOM CYLINDRICAL SHELL TANKS SUBJECTED TO HORIZONTAL SINOSOIDAL GROUND MOTION

Tomoyo Taniguchi
Tottori University, Department of Civil Engineering
4-101 Koyama-Minami Tottori, 680-8552, Japan
Telephone +81-857-31-5287, Fax +81-857-28-7899,
E-mail t_tomoyo@cv.tottori-u.ac.jp

Koji Imai
Tottori University, Department of Civil Engineering
4-101 Koyama-Minami Tottori, 680-8552, Japan
Telephone +81-857-31-5288, Fax +81-857-31-5288,
E-mail imai@str.cv.tottori-u.ac.jp

ABSTRACT

The governing equations of motion of walking phenomena of unanchored flat-bottom cylindrical shell tanks subjected to horizontal sinusoidal ground motion are examined. The equations of motion are derived through variational approach. The physical quantities related to the walking phenomena are the mass of tank itself, tank content, the effective mass of liquid for bulging motion, that for rocking motion, that for rocking-bulging interaction motion, and friction force including self-weight reduction effects. The roles of each physical quantity during the walking motion are clearly identified. Comparison of the time history of experimental results and that of analytical ones corroborates accuracy of the proposed equations of motion.

INTRODUCTION

The large slip of a flat bottom cylindrical shell tank was observed when the tank experienced severe ground motion [1, 2]. Although the phenomenon has been called "walking," to the writer's knowledge, there are few research concerned with this topic.

Kobayashi [3] presented a multi-degree-of-freedom model for the large slip of the tank, which models the fluid-structure interaction and uplift of the tank. However, its applicability is not thoroughly discussed. In contrast, the senior author [4] presented the mechanical model to analyze the rocking motion of the tank based on the analogy with the rocking dynamics of the rectangular rigid bodies [5]. Its accuracy is confirmed by comparing computation results with experimental ones. Keys to the problem concerned here are the rocking-bulging interaction and self-weight-lightening effects. As its expansion, the companion paper [6] reveals that the walking motion of tanks can be explained in view of bulging-rocking-slip interaction motion. The mechanical model for the waking motion of the model tank is formulated. Its accuracy is confirmed by comparison of experiment results of walking motion subsequent to releasing the initial enforced uplift angle with numerical ones.

Therefore, this research tries to confirm applicability of the previously proposed mechanical model under action of horizontal shaking. To simplify the problem, this study assumes that the uplift region of the bottom plate is the concentric doughnuts shape (see Fig. 2a), although the actual tanks have crescent-like uplift region [7]. This simplification enables to account the effective mass of liquid for rocking motion clearly. The effective mass of liquid for rocking motion distributes along the filling height of contents and from inward shell plate up to the edge of rigid-doughnuts-shape bottom plate. The appearance of the effective mass of liquid for rocking motion can be regarded as the concentric hollow cylinder. The wall thickness of the concentric hollow cylinder is the same as the width of the rigid-doughnuts-shape bottom plate, (see Fig. 2b). The rigid-doughnuts-shape bottom plate guarantees the reciprocal motion of the concentric hollow cylinder accompanied with the rocking motion of the tank. In addition, the moment inertia of the entire tank system is represented by the effective mass of liquid for rocking motion.

The liquid is assumed incompressive, Newtonian fluid and fluid displacements are assumed small.

SCENARIO TO WALKING

Our series researches presume that the walking behavior of tanks may follow the rocking response of tanks, since the rocking response of tank lightens its arbitrary self-weight [4]. The base shear of the tank and the friction between the underside of the bottom plate of the tank and the surface of the foundation directly concern with the slip behavior. Although the self-weight-lightening effects reduce the friction, it is considered as a remote cause. In addition, the bulging response induces the rocking response of tanks. Figure 1 shows the

schematic diagram of the scenario to walking phenomenon. The following discussion is pursued based on this scenario.

DYNAMICS OF TANK MODEL

The authors derived governing equations of motion of walking behavior of model tank without external force term and confirmed its accuracy by the motion subsequent to releasing the initial enforced uplift angle [6]. Therefore, governing equations of motion for walking behavior of the tank subjected to horizontal shaking is given by adding external force term regarding the inertia force to the aforementioned equations. Figures 2a to 2c depict definition of coordinates.

Rotational direction

$$\begin{aligned}&(I_E+I_S)\ddot{\theta}-\{\lambda M_I R_I\cos(\alpha_I-\theta)+M_I x_I\sin\theta+\lambda M_S R_S\cos(\alpha_S-\theta)\}\ddot{x}\\&+g\{M_E R_0\sin(\alpha_0-\theta)+M_S R_S\sin(\alpha_S-\theta)+\lambda M_{rb}x_I\cos\theta\}\\&+2M_{rb}(x_I+\lambda R_I\sin\alpha_I)\dot{x}_I\dot{\theta}-\lambda M_I R_I\cos\alpha_I\,\ddot{x}_I\\&-M_I\{x_I\sin\theta+\lambda R_I\cos(\alpha_I-\theta)\}\ddot{z}_h=0\end{aligned} \tag{1}$$

Translational direction of the bulging motion

$$\begin{aligned}&M_I\ddot{x}_I+\lambda M_{rb}g\sin\theta-\lambda M_{rb}R_I\sin\alpha_I\,\dot{\theta}^2-\lambda M_{rb}R_I\cos\alpha_I\,\ddot{\theta}\\&+M_I\cos\theta\,\ddot{x}-M_{rb}\dot{x}\sin\theta\,\dot{\theta}-M_{rb}x_I\dot{\theta}^2+M_I\cos\theta\,\ddot{z}_h+kx_I+c\dot{x}_I\\&=0\end{aligned} \tag{2}$$

Translational direction of the tank slip

$$\begin{aligned}&(M_I+M_S)\ddot{x}+M_I\cos\theta\,\ddot{x}_I-2M_{rb}\sin\theta\,\dot{x}_I\dot{\theta}+(M_I+M_S)\ddot{z}_h\\&-\{M_{rb}x_I\sin\theta+\lambda M_E R_0\cos(\alpha_0-\theta)+\lambda M_S R_S\cos(\alpha_S-\theta)\}\ddot{\theta}\\&-\{M_{rb}x_I\cos\theta+\lambda M_E R_0\sin(\alpha_0-\theta)+\lambda M_S R_S\sin(\alpha_S-\theta)\}\dot{\theta}^2\\&=-F\end{aligned} \tag{3}$$

Friction force

$$\begin{aligned}F=\nu\,sign(\dot{x})\big[&M_T g-\lambda M_I\sin\theta\,\ddot{x}_I-M_{rb}x_I\sin\theta\,\dot{\theta}^2+M_{rb}x_I\cos\theta\,\ddot{\theta}\\&+2M_{rb}\cos\theta\,\dot{x}_I\dot{\theta}-\{M_E R_0\cos(\alpha_0-\theta)+M_S R_S\cos(\alpha_S-\theta)\}\dot{\theta}^2\\&+\{M_E R_0\sin(\alpha_0-\theta)+M_S R_S\sin(\alpha_S-\theta)\}\ddot{\theta}\big]\end{aligned} \tag{4}$$

Whereas I_E, I_S: moment inertia of the effective mass of liquid for rocking motion and tank itself including the bottom plate uplifted, M_I, M_E, M_{rb}, M_S: effective mass for bulging motion, that for rocking motion, that for rocking-bulging interaction motion and the mass of the tank itself including the bottom plate uplifted, R_0, R_I, R_S: distance from the gravity center of M_E, that of M_{rb}, that of M_S to the pivoting edge O or O'. When the tank is at rest, the lines R_0 and R_I make the angles α_0 and α_I with the vertical, respectively. The value of M_I and natural period of the first bulging mode can be determined based on the seismic design code [8]. Moreover, since M_S and I_S is relatively small to M_E and I_E, these can be negligible. ν is the kinetic friction coefficient.

Here, the index λ is introduced to unify the expressions and specifies the rotational direction. The value of λ is 1 when the model pivots on the left bottom edge (around O), and is –1 when it does on the right bottom edges (around O'). λ changes its sign every landing of either bottom edges.

Rocking commencement condition

$$m_E gR_0\sin\alpha_0 < m_I\left|\ddot{x}_I\right|H_I+m_T\left|\ddot{x}+\ddot{z}_h\right|R_0\cos\alpha_0 \tag{5}$$

The value of λ at the onset of rocking motion is;

$$\lambda=1 \quad \text{if} \quad \ddot{x}+\ddot{x}_I+\ddot{z}_h>0 \tag{6a}$$

$$\lambda=-1 \quad \text{if} \quad \ddot{x}+\ddot{x}_I+\ddot{z}_h<0 \tag{6b}$$

The slip commencement condition can be determined by balance between static friction force and base shear.

Slip commencement condition

$$\left|R_x\right|>\mu R_y \tag{7}$$

Whereas μ is the static friction coefficient. R_x and R_y are base shear and normal reaction on the general coordinate, respectively. It is noted that these force should include effects of rocking motion.

$$\begin{aligned}R_x=&M_I\cos\theta\,\ddot{x}_I-M_{rb}x_I\cos\theta\,\dot{\theta}^2-M_{rb}x_I\sin\theta\,\ddot{\theta}+(M_I+M_S)\ddot{z}_h\\&-\lambda\{M_E R_0\sin(\alpha_0-\theta)+M_S R_S\sin(\alpha_S-\theta)\}\dot{\theta}^2\\&-\lambda\{M_E R_0\cos(\alpha_0-\theta)+M_S R_S\cos(\alpha_S-\theta)\}\ddot{\theta}\end{aligned} \tag{8}$$

$$\begin{aligned}R_y=&M_T g-\lambda M_I\sin\theta\,\ddot{x}_I-M_{rb}x_I\sin\theta\,\dot{\theta}^2+M_{rb}x_I\cos\theta\,\ddot{\theta}\\&-\{M_E R_0\cos(\alpha_0-\theta)+M_S R_S\cos(\alpha_S-\theta)\}\dot{\theta}^2\\&+\{M_E R_0\sin(\alpha_0-\theta)+M_S R_S\sin(\alpha_S-\theta)\}\ddot{\theta}\end{aligned} \tag{9}$$

In addition, the transition from the liftoff around an edge to the liftoff around another one is accompanied by an impact. The associated energy loss is accounted for by reducing the angular velocity of the body after impact. Specifically, it can be expressed as follows in compliance with law of conservation of momentum.

$$\dot{\theta}(t^+)=e\dot{\theta}(t^-) \qquad 0\le e\le 1 \tag{10}$$

Whereas e is coefficient of restitution; t^+ is the time just after impact; t^- is the time just before impact. Although the duration of impact was measured at free liftoff motion tests [9], it is ignored in this study. Changes in angular velocity are considered to occur instantaneously.

RESULTS AND DISCUSSIONS

The acrylic model tank, whose diameter and height is 400 mm each and shell thickness is 10 mm, with rigid full bottom plate (10 mm in thickness) is examined. The tank contains M_0=50.3 kg water, forms 26 Hz bulging system (fluid-elastic shell interaction) and is assumed to have 5% damping ratio. The ratio of effective mass for bulging motion to the all mass of tank contents M_I/M_0 is 0.782 [8]. R_0, R_I, α_0 and α_I are 0.283m, 0.258m, 0.785rad and 0.889rad, respectively. In this case, since all bottom plate effectively works for rocking

motion, the effective mass for rocking motion is the same as the all mass of the tank contents. Therefore, M_E and I_E are 50.3kg and 5.198m^4, respectively. The coefficient of static friction is assumed as μ=0.2, while the coefficient of kinetic friction is assumed as 95% of that of static coefficient. The coefficient of restitution is assumed as e=0.6.

The model tank is set on the shaking table which can impose 7Hz horizontal sinusoidal acceleration with maximum acceleration 20m/s^2.

Figure 4a shows horizontal acceleration records of the shaking table. Since the experimental records contains some high frequency components, the smoothed sinusoidal acceleration is used in the analysis. In addition, only stationary response is considered. All numerical simulation are performed by commercial numerical integration package ACSL [10]. Figures 4b and 4c compare the experimental uplift angle and slip displacement with those of analytical ones, respectively. The solid line in each graph shows the experimental results, while those of the bold line presents the analytical ones. Although the restitution and friction conditions may vary place by place, the analytical results well simulates the experimental ones.

Finally, the acrylic tank with 10% rigid-doughnuts bottom plate model is examined (δ=0.9). The center part of the bottom plate is covered with mass-less and stiffness-less membrane to prevent leaking the water (see Fig. 2a). The dimension of the tank is the same as the tank used in the aforementioned examination. In this case, since the partial bottom plate effectively works for rocking motion, the effective mass for rocking motion and rocking-bulging interaction should be considered. In this condition, the ratio of the effective mass for rocking-bulging interaction to the one for bulging motion, M_{rb}/M_I, is given as 0.152 (see Fig. 3). M_E and I_E are 9.56kg and 1.065m^4, respectively. The coefficient of static friction is assumed as μ=0.2, while the coefficient of kinetic friction is assumed as 95% of that of static coefficient. The coefficient of restitution is assumed as e=0.6.

Figure 5a shows horizontal acceleration of the shaking table recorded and the smoothed sinusoidal acceleration used in the analysis. Figures 5b and 5c compare the experimental uplift angle and slip displacement with those of analytical ones, respectively. The solid line in each graph shows the experimental results, while those of the bold line presents the analytical ones. Although the restitution and friction conditions may vary place by place, the analytical results well simulates the experimental ones.

These results indicate that the mechanism presented herein is applicable to analyze the waking motion of tanks despite the extent of the uplift region of the bottom plate of tanks.

CONCLUSION

Employing horizontal sinusoidal shaking tests, this paper examines the fundamental mechanics of the walking behavior of the flat-bottom cylindrical shell tanks during the earthquake. The results indicate that walking behavior of tanks can be described by equations of motion including bulging-rocking-slip interaction motion. All physical quantities needed for analysis are clarified.

ACKNOWLEDGMENTS

The authors express their sincere thanks to Mr. Yoshihiro Shiroo and Kenichiro Kawami, Kawajyu Technoservive, Ltd. and Mr. Yoshinori Ando, Graduate student of Tottori University for their dedication to accurate experimental work and the collection of much valuable data.

REFERENCES

[1] Rinne, J. E., 1967, “Oil Storage Tanks, The Prince William Sound, Alaska, Earthquake of 1964 and aftershocks”, U. S. Department of Commerce Environmental Science Service Administration, pp. 245-252.

[2] Steinverge, K. V., 1970, “Earthquake Damage and Structural Performance in the United States, Earthquake Engineering”, Prentice-Hall, Inc., pp. 209-221.

[3] Kobayashi, N. Ito, M. Watanabe M. Tazuke, H. “Nonlinear Analysis on Rocking and Sliding Coupled Response of Cylindrical Tank Due to Seismic Excitation,” JSME(C), 2002; 68-666(2): 357-364. (Japanese)

[4] Taniguchi, T. “Rocking dynamics of unanchored model flat-bottom cylindrical shell tanks subjected to harmonic excitation,” Journal of Pressure Vessel Technologies, ASME, Vol. 127, Issue 4, pp. 373-386, 2005.

[5] Taniguchi, T. “Nonlinear response analysis of rectangular rigid bodies subjected to horizontal and vertical ground motion”, Journal of Earthquake Engineering and Structural Dynamics, Volume 31, Issue 8, pp. 1481-1500, 2002.

[6] Taniguchi, T. Imai, K. “Governing equations of motion of walking behavior of unanchored flat-bottom cylindrical shell model tanks,” PVP, Seismic Engineering, ASME, Paper No. PVP2005-71288, 2005.

[7] Clough, D. P., 1977-5, “Experimental Evaluation of Seismic Design Method for Broad Cylindrical Tanks”, Univ. of California, EERC Rep., No. UCB/EERC-77/10.

[8] MITI Notification No. 515, issued Oct. 26, 1981.

[9] Taniguchi, T. “Experimental and analytical study of free lift-off motion induced slip behavior of rectangular rigid bodies,” Journal of Pressure Vessel Technologies, ASME, Vol. 126, Issue 1, pp. 53-58, 2004.

[10] ACSL Reference Manual, Edition 11.1, 1995, MGA Software.

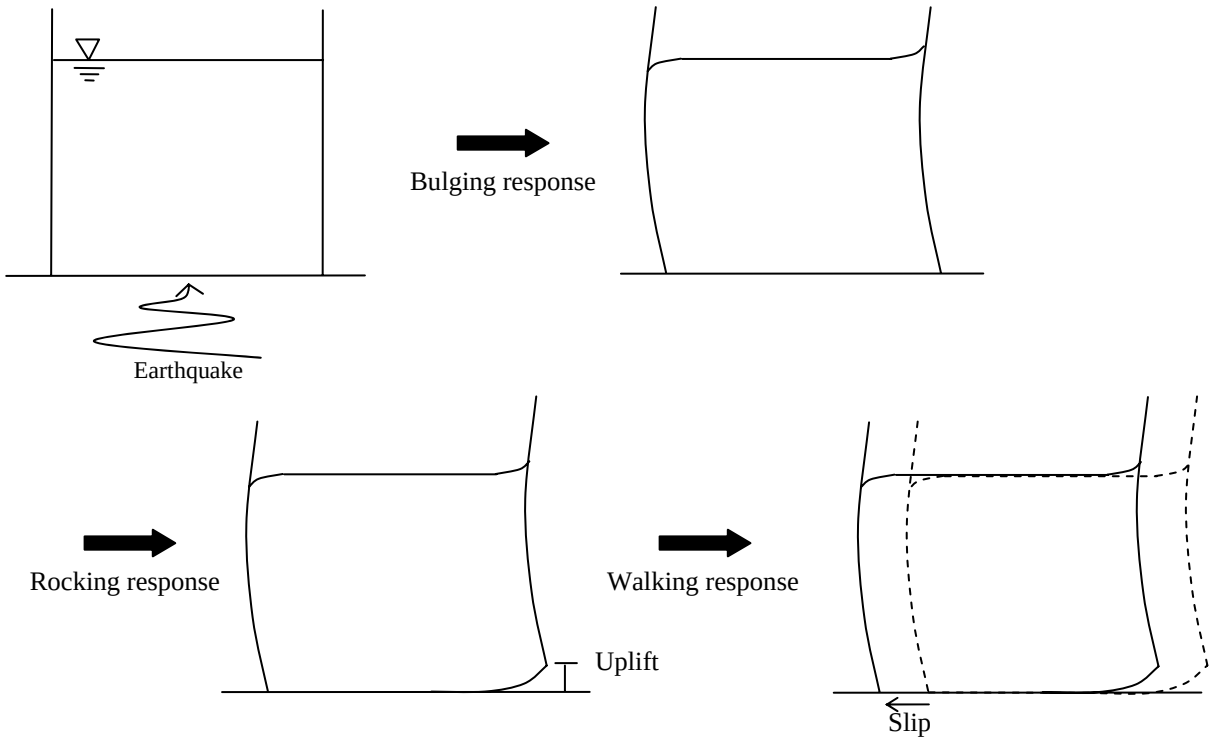

Figure 1 Scenario to walking behavior of tanks

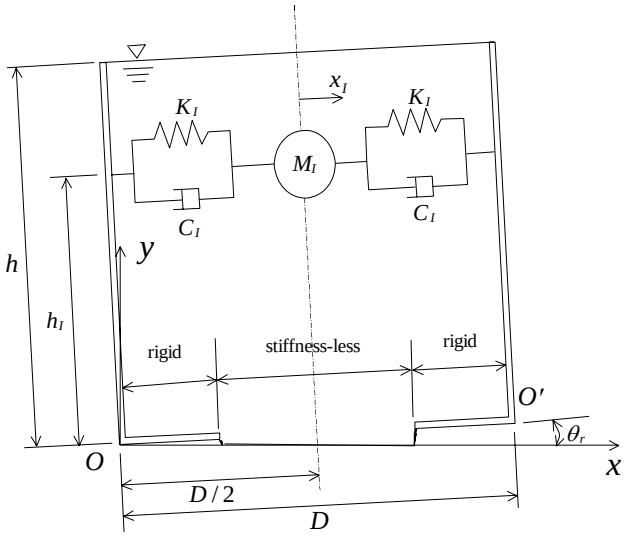

Figure 2a Schematic representation of the tank model

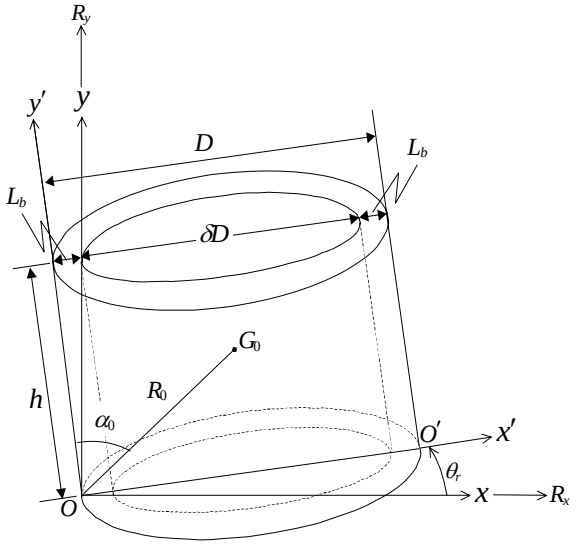

Figure 2b Schematic distribution of effective mass for rocking motion M_E (L_b: Uplift width of bottom plate)

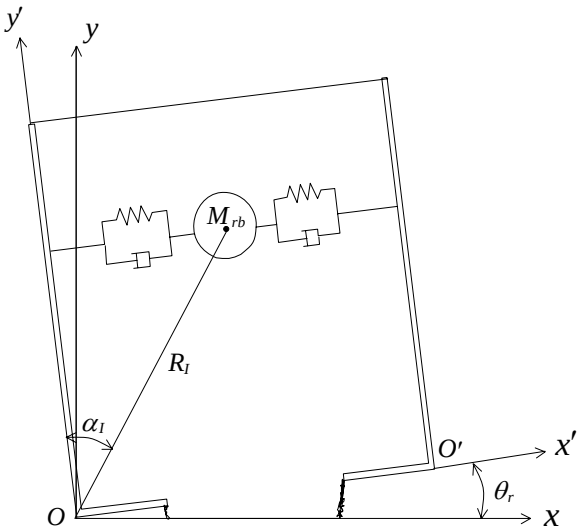

Figure 2c Schematic representation of effective mass for rocking bulging interaction motion M_{rb}

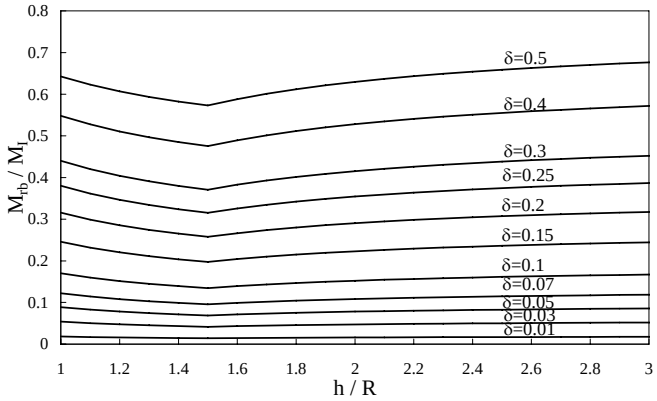

Figure 3 Ratio of effective mass of liquid for rocking-bulging interaction motions to that for impulsive mass [4]

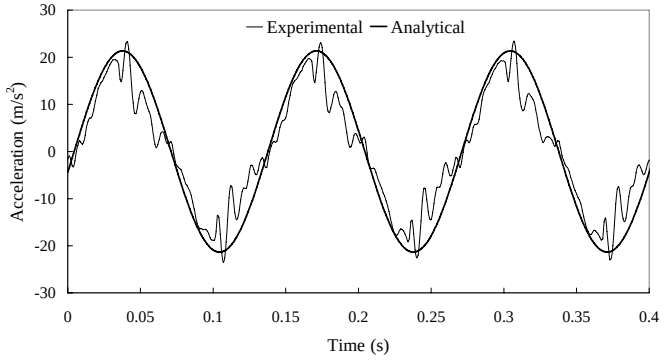

Figure 4a Horizontal acceleration of shaking table (rigid full bottom plate)

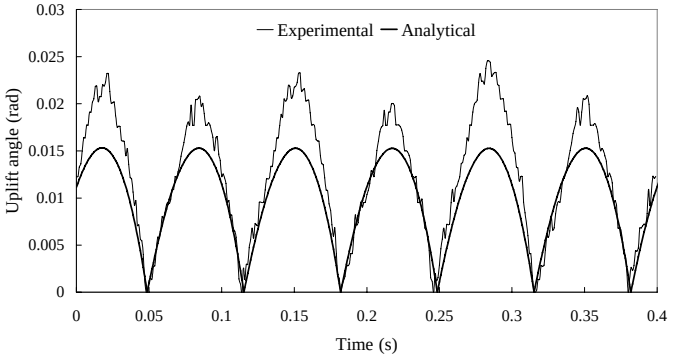

Figure 4b Uplift angle of tank (rigid full bottom plate)

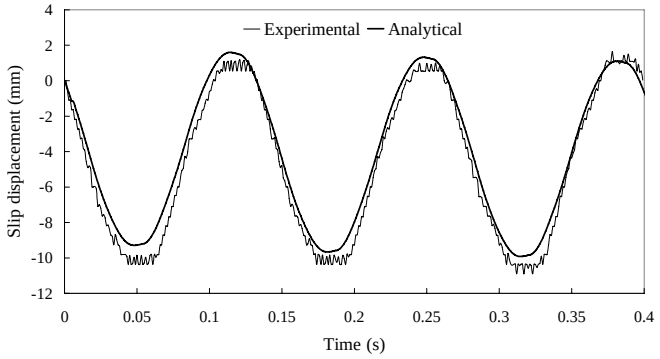

Figure 4c Slip displacement of tank (rigid full bottom plate)

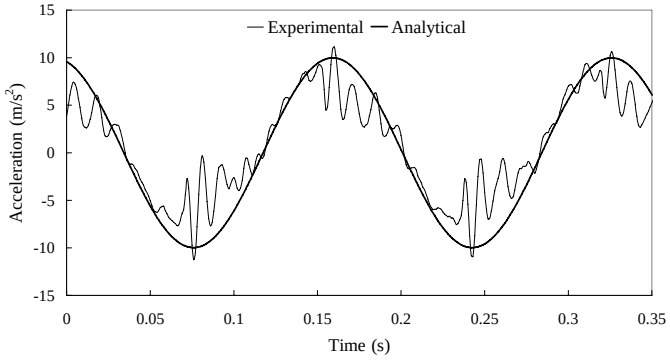

Figure 5a Horizontal acceleration of shaking table (10% rigid-doughnut bottom plate)

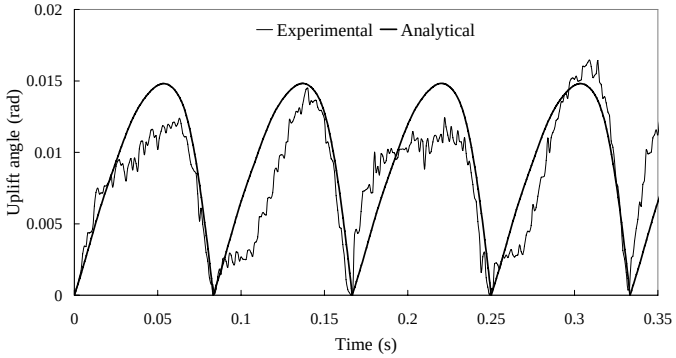

Figure 5b Uplift angle of tank (10% rigid-doughnut bottom plate)

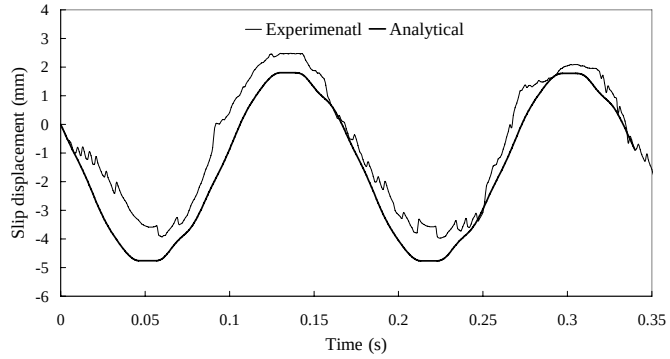

Figure 5c Slip displacement of tank (10% rigid-doughnut bottom plate)